

Tensile Stress Measurements on Linear and Branched Low-Density Polyethylene Melts. Interpretation of Results with a Generalized Maxwell Model

R. MULLER, J. L. BAREA and P. SANSEAU, *Institut Charles Sadron (CRM-EAHP), 4, rue Boussingault, Strasbourg, France*

Synopsis

Dynamic shear experiments in the linear range of deformation and extensional tests at constant strain rate have been carried out on a linear low-density polyethylene (LLDPE) melt and on two branched low-density polyethylene (LDPE) melts with different amounts of long-chain branching. Both the dynamic shear moduli and the tensile stress obey the time-temperature superposition principle. A simple model based on a nonaffine generalized Maxwell model with two relaxation times is proposed to describe the rheological behavior in elongation of these melts. Close agreement between the model and the experimental data can be obtained by adjusting the two relaxation times and the "slip parameter" of entanglements. The variations of these parameters with strain rate and their relationship with molecular structure are discussed.

INTRODUCTION

Among all polyolefines, low-density polyethylene holds a prominent industrial position. On account of its diversity (it may be used in film extrusion, foam extrusion, wire coating, etc.) different grades have been developed with their rheological behavior adapted to the different processing methods.

It is well established¹ that molecular weight distribution and extent of long-chain branching are the determining parameters in the rheology of polyethylene melts. Over the past few years, a new variety of low-density polyethylene, linear low-density polyethylene (LLDPE), has begun to compete with low-density polyethylene polymerized by free radical mechanism (LDPE) in the field of films, mainly due to desirable mechanical properties of the end product and an improved processability of the polymer melt. From a molecular point of view, LLDPE is a linear molecule with a great number of short branches, contrary to LDPE which is constituted of long-chain branched molecules. It could be shown that the rheological behavior in shear of LLDPE is fairly different from that of LDPE.^{2,3}

However, shear rheology and linear viscoelastic properties are often inadequate to predict the processability of a polymer melt. In many processes, the deformation experienced by the material includes a large elongational component. This explains the growing interest for elongational viscosity measurements of polymer melts.⁴⁻⁶ Generally, it is difficult to determine the elongational rheological behavior from the shear properties⁷ and this has to be measured separately.

From an experimental point of view, this type of test is much more tricky to realize than shear measurements such as cone and plate or capillary rheometry. Yet, several studies have been published and experimental data in the field of elongational rheology have been communicated for various LDPE and LLDPE melts.^{6,8}

As expected, molecular weight distribution and structure of chains, especially the number and the length of branches, affect elongational rheology as in shear, and notable differences in behavior of LDPE and LLDPE have been observed.^{8,9}

Further to the experimental problems arising from tensile viscosity measurements necessitating specific apparatus, molding and fastening of specimens, the lack of a simple model describing the rheology of polymer melts in this type of deformation renders experimental results difficult to exploit. In this paper, we measured both the dynamic viscoelastic properties in the linear range and the tensile stress-growth coefficient at different strain rates for three LDPE samples: one LLDPE and two LDPE samples branched to different extents. We then tried to account for the elongational rheology results with a rather simple model based on a generalized Maxwell model with two relaxation times.

EXPERIMENTAL METHODS

Polymer Samples

Three polyethylene samples from the CdF Chimie Company have been studied; their molecular characteristics are shown in Table I. The first two polymers are LDPE samples called LD1 and LD2 with different molecular weight distribution and long-chain branching extent. The LD2 polymer has a higher polydispersity than the LD1 sample, whereas the long-chain branching of LD2 is lower than that of LD1. The third sample, LL1, is a LLDPE with an average molecular weight close to that of LD2.

Dynamic Shear Rheology

The dynamic moduli and viscosities of these three samples have been measured as a function of frequency at two temperatures (150°C and 180°C) with a Rheometrics RMS 605 mechanical spectrometer. The amplitude of the sinusoidal strain was small enough (< 5%) so that the behavior of the melt was linear viscoelastic.

The dynamic moduli G' and G'' have been plotted as a function of frequency at 150°C in Figure 1. The corresponding curves at 180°C can be exactly superimposed on to that obtained at 150°C by a simple translation on the frequency axis. The value of the shift factor $\log(a_T)$ is shown in Table II for the three samples.

Figure 2 shows the so-called "Cole-Cole diagrams" of the complex viscosity (i.e., η'' as a function of η'). For the LD1 and LL1 samples, the extrapolation of the curves allows a precise determination of their intersection with the η' axis and therefore of the zero shear viscosity of the melt. For the LD2 sample, this extrapolation is more difficult; nevertheless, it allows an approximate

TABLE I
Melt Flow Index (MFI), Molecular Weight Distribution and Long-Chain Branching Extent
(Number of Ternary Carbon Atoms for 1000 Carbons) of the Three Melts Studied

	MFI	M_n	M_w	M_w/M_n	Long-chain branching
LD1	1.05	23,000	122,000	5.4	5.3
LD2	0.16	20,000	146,000	7.2	2.5
LL1	0.9	28,000	146,000	5.3	17.7

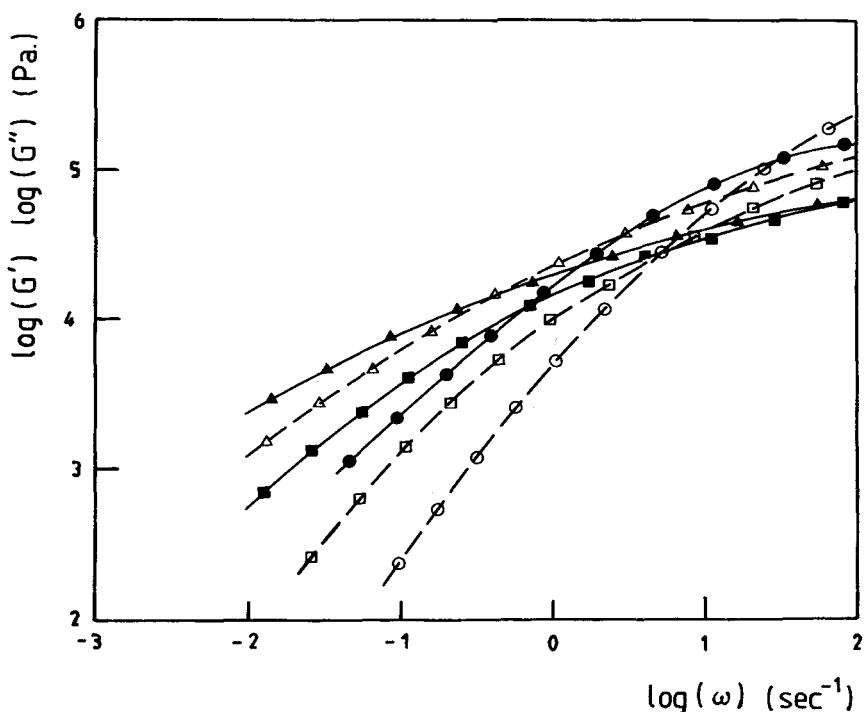


Fig. 1. Storage modulus G' (---) and loss modulus G'' (—) for the three melts at 150°C: (○, ●) LL1; (□, ■) LD1; (△, ▲) LD2.

estimation of η_0 . Figure 3 represents the variations of the dynamic viscosity $\eta^* = (\eta'^2 + \eta''^2)^{0.5}$ as a function of frequency for the three melts.

The values of zero-shear viscosity at 150°C as well as the values of η^* at the same temperature for several values of the frequency are shown in Table II. As will be seen later, these data will be useful for the correlation of tensile stress-growth measurement with the linear viscoelastic measurements.

Elongational Rheology

The deformation of the polymer melt specimen should be regular during the carrying out of a tensile stress-growth measurement. This leads to the fabrication of perfectly homogeneous specimens that are free of any residual orientation at the end of the molding process. Compression molding of pellets does

TABLE II

Thermal Shift Factor $\log(a_T)$ Between 150 and 180°C; Zero Shear Viscosity at 150°C and Dynamic Viscosity in Pa · s at the Same Temperature for Different Values of the Frequency (ω in rad/s)

	$\log(a_T)$	η_0 Pa · s	η^* (.03)	η^* (.055)	η^* (.11)	η^* (.22)	η^* (.52)	η^* (1)
LD1	.44	5.8E4		4.4E4	3.7E4		2.3E4	1.7E4
LD2	.47	6.0E5	1.7E5	1.3E5	9.7E4	7.1E4	4.3E4	2.9E4
LL1	.27	2.5E4			2.3E4		2.0E4	1.8E4

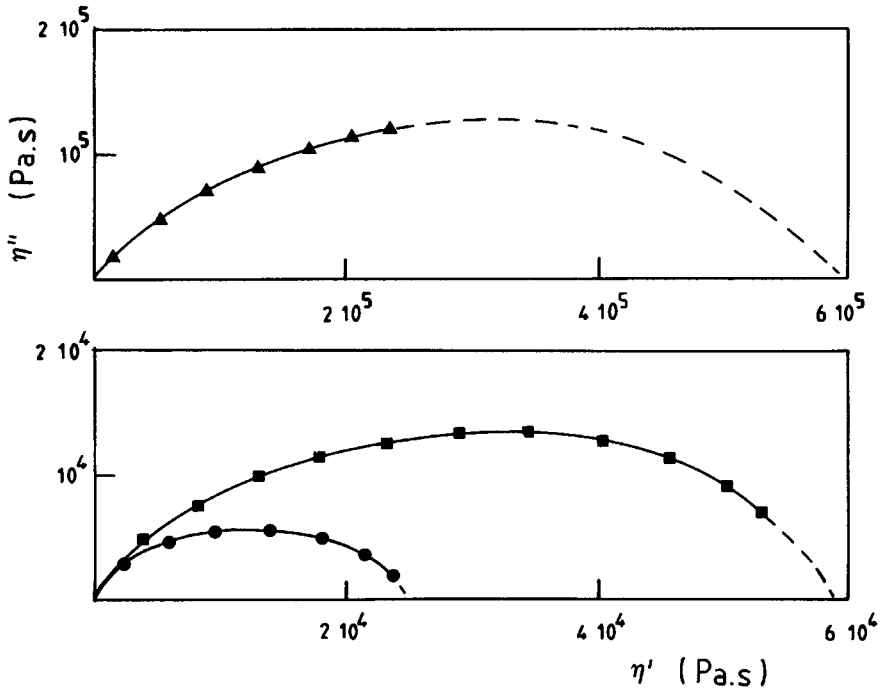


Fig. 2. Cole-Cole plots of the complex viscosity for the three samples: (●) LL1; (■) LD1 (▲) LD2. Extrapolation of the experimental data with a circular regression (----) for the determination of the zero shear viscosity.

not satisfy the first requirement of homogeneity and leads to an irregular deformation of the melts. Therefore, the transfer molding technique was used, which gives a satisfactory homogenization of the polymer and does not require large amounts of material. However, this method does not allow a sufficient relaxation of the internal stresses due to the high cooling rate in the mold. The specimens obtained in that way deform as soon as they are heated above the melting temperature. Here again, the deformation during the extensional test is irregular and leads to useless results.

In order to relax this residual orientation, the molded specimens had to be annealed above the melting temperature with the device shown in Figure 4. The transfer-molded parallelepipeds are placed between two iron plates pressed together with springs. The whole device is then immersed in a silicone oil bath

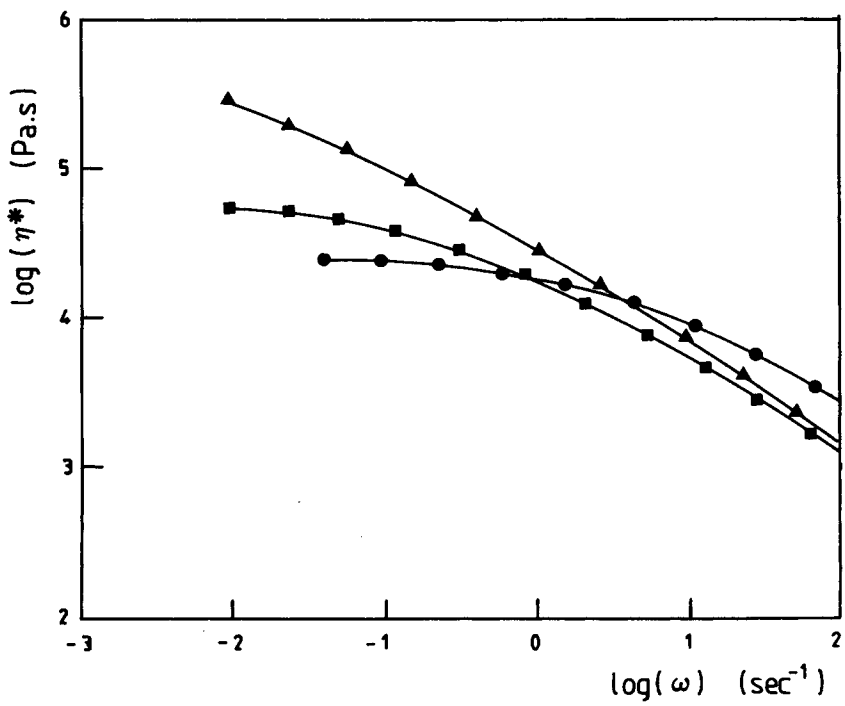


Fig. 3. Dynamic viscosity $\eta^* = (\eta'^2 + \eta''^2)^{0.5}$ as a function of frequency: (●) LL1; (■) LD1; (▲) LD2.

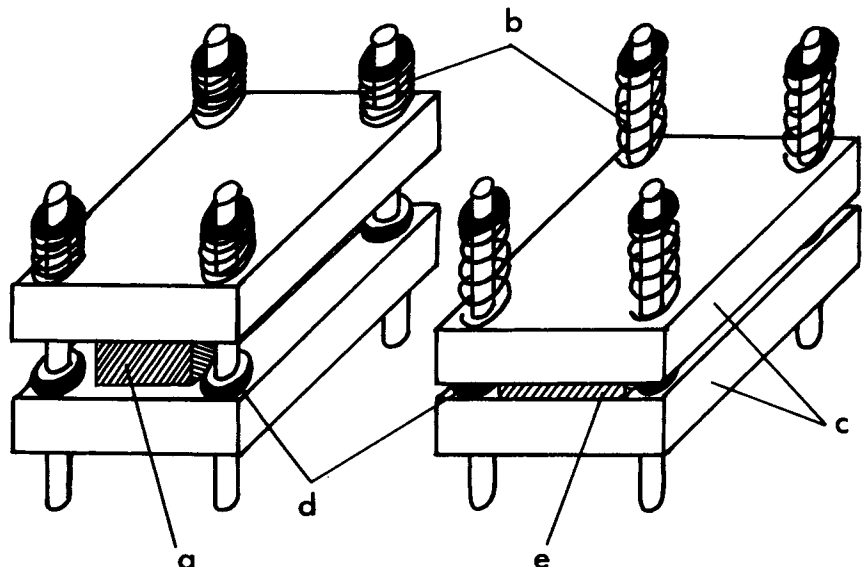


Fig. 4. Experimental device for annealing the transfer molded specimens above the melting temperature (a) transfer-molded specimen, (b) springs, (c) plates, (d) o-rings, (e) molten specimen during annealing.

at 180°C. Once the polymer melts, the plates squeeze the specimen and come in contact with small *o*-rings yielding a constant final thickness of the specimen. Then one only has to wait for a time long enough compared to the terminal relaxation time of the melt (about 10 to 20 minutes for the three LDPE samples under consideration). Finally the specimens used for the elongation rheology measurements are machined after cooling in the polymer plates thus obtained.

The elongational measurements have been carried out with an apparatus designed in this laboratory, of which a detailed description has been published.¹⁰ A device for fastening the melt specimens made of small self-blocking clamps has been realized and has proved to be particularly convenient for polyolefine melts as it avoids all gluing problems. This extensional rheometer is now manufactured by the METRAVIB R.D.S Company (Ecully, France).

Figure 5 shows the tensile stress-growth coefficient of the three melts as a function of time for various strain rates and at 150°C. One observes that only LL1 melt reaches a steady-state regime for the lowest strain rate. If the value of the steady-state tensile viscosity which can be defined under these conditions ($\eta_E(\dot{\epsilon}) = 8.10^4 \text{ Pa} \cdot \text{s}$), is compared to the zero shear viscosity η_0 of the LL1 melt at the same temperature (cf. Table II), it can be observed that the value of η_E is equal to about three times that of η_0 , which amounts to say that Trouton's relation is verified with a good approximation.^{9,11}

In order to check the reliability of our results, we carried out a second series of measurements at a higher temperature ($T = 180^\circ\text{C}$). We then compared for

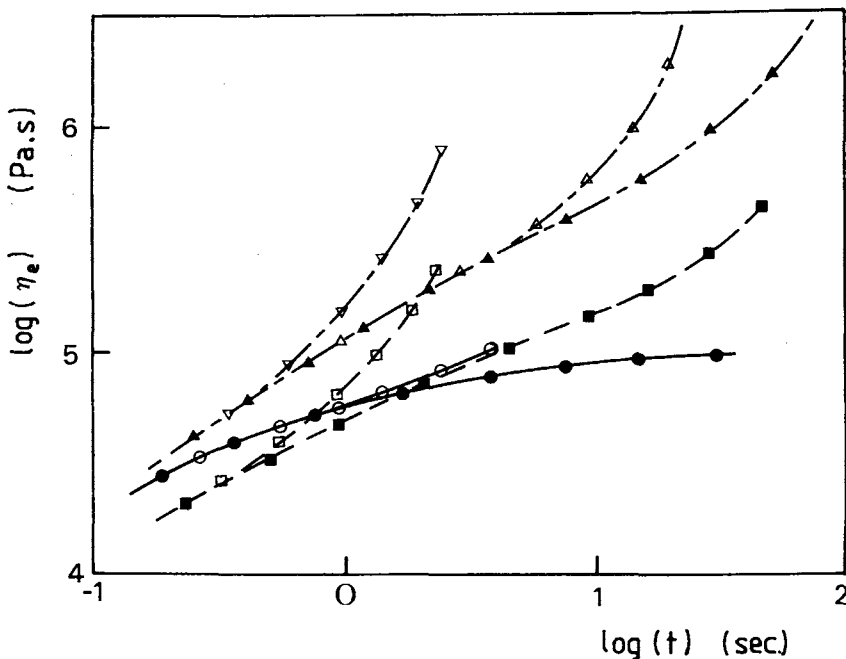


Fig. 5. Tensile stress-growth coefficient as a function of time at 150°C and different strain rates: (—) LL1: (●) 0.1 s^{-1} ; (○) 1 s^{-1} ; (-----) LD1: (■) 0.05 s^{-1} ; (□) 1 s^{-1} ; (.....) LD2: (▲) 0.05 s^{-1} ; (△) 1 s^{-1} ; (▽) 1 s^{-1} .

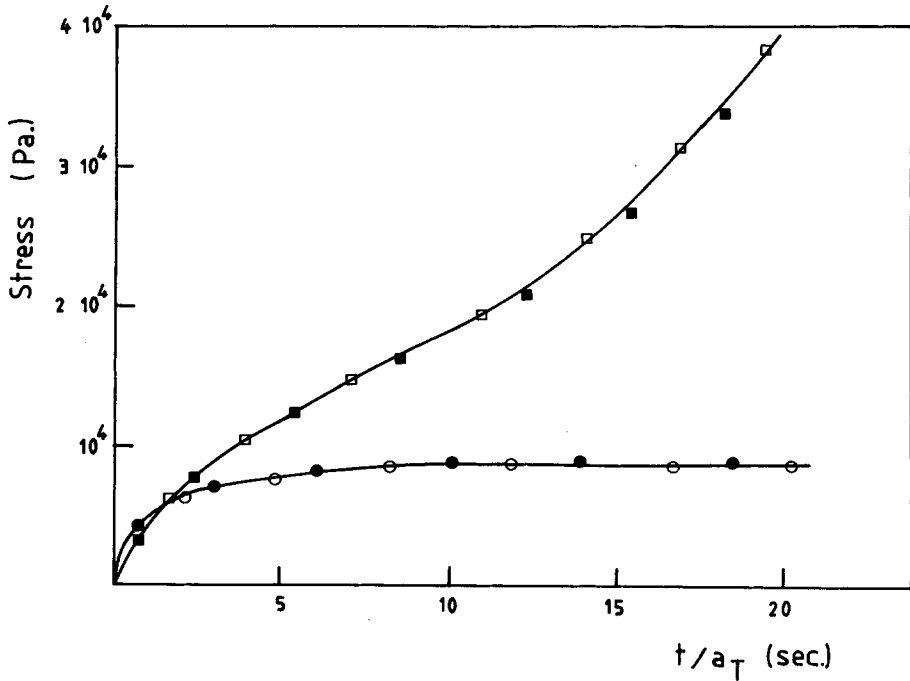


Fig. 6. Tensile stress versus reduced time for two different temperatures: (●, ○) LL1; (●) $T = 150^\circ\text{C}$, $\dot{\epsilon} = .1 \text{ s}^{-1}$; (○) $T = 180^\circ\text{C}$, $\dot{\epsilon} = .19 \text{ s}^{-1}$; (■, □) LD1; (■) $T = 150^\circ\text{C}$, $\dot{\epsilon} = .1 \text{ s}^{-1}$; (□) $T = 180^\circ\text{C}$, $\dot{\epsilon} = .27 \text{ s}^{-1}$.

the three polymers the tensile stress for two tests run at 150°C and 180°C respectively with strain rates $\dot{\epsilon}_0$ and $\dot{\epsilon}_0/a_T$ where a_T is the thermal shift factor determined from the linear viscoelasticity measurements (see Table II). Figures 6 and 7 represent the tensile stress as a function of reduced time for five pairs of comparable tests on the three melts. Our extensional rheology results agree with those of Münstedt and Laun on a branched LDPE melt¹² and our previous study on a polystyrene melt;¹⁰ they show that the time-temperature equivalence principle is verified independently of the structure of the polymer (i.e., whether it is a short- or long-chain branching).

PROPOSED MODEL

The so-called quasilinear viscoelastic models form a class of rheological models which have been used successfully to describe the rheological behavior of polymer melts. Their general expression is:

$$\sigma(t) = \int_{-\infty}^t m(t-t')\mathbf{S}_i(t') dt' \quad (1)$$

Where σ is the stress tensor and \mathbf{S} a nonlinear strain tensor. The quantity m is the memory function which can be obtained from linear viscoelastic

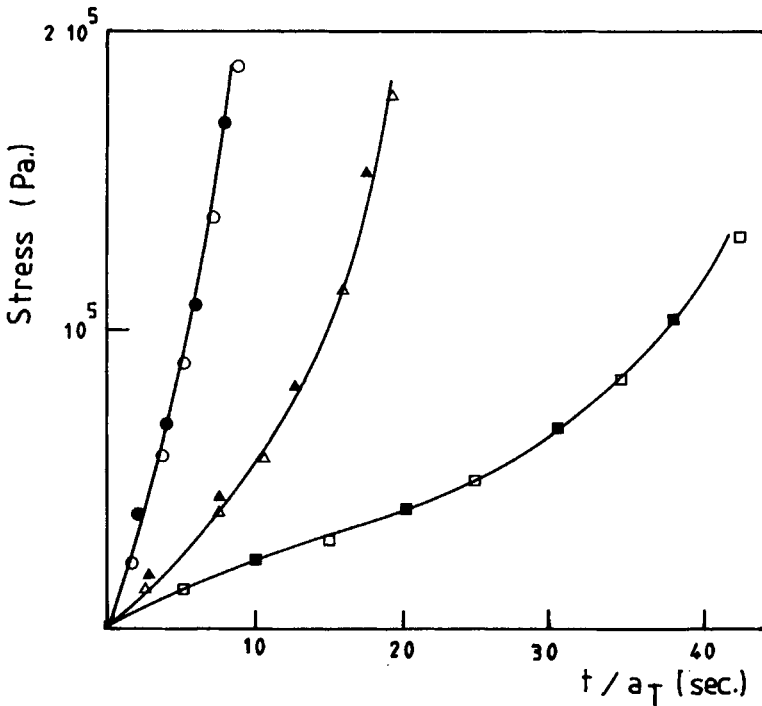


Fig. 7. Tensile stress versus reduced time for the LD2 melt at 150°C (■, ●, ▲) and 180°C (□, ○, △): (■) $\dot{\epsilon} = .05 \text{ s}^{-1}$; (□) $\dot{\epsilon} = .148 \text{ s}^{-1}$; (●) $\dot{\epsilon} = .1 \text{ s}^{-1}$; (○) $\dot{\epsilon} = .3 \text{ s}^{-1}$; (▲) $\dot{\epsilon} = .2 \text{ s}^{-1}$; (△) $\dot{\epsilon} = .59 \text{ s}^{-1}$.

measurements. If G is the relaxation modulus of the material, we have:

$$m(s) = - \frac{dG(s)}{ds} \quad (2)$$

Depending on the choice of the strain tensor \mathbf{S} , different types of models can be obtained. If one considers the Finger strain tensor \mathbf{C}^{-1} , the rubberlike liquid model of Lodge is obtained by taking $\mathbf{S} = (\mathbf{C}^{-1} - \mathbf{I})$ where \mathbf{I} is the identity tensor. More complex choices for \mathbf{S} lead, for example to the Wagner model⁷ as well as to the Doi-Edwards model.¹³

Another alternative developed by Tschoegl¹⁴ and Johnson and Segalman¹⁵ consists in assuming that the deformation of the network of junction points between the chains (i.e., entanglements) is not affine and to introduce a slip parameter α equal to 1 in the affine assumption, which is generally between 0 and 1 for polymeric fluids. It can then be shown that in the case of a uniaxial extensional flow, the corresponding strain tensor \mathbf{S} can be written as:¹⁶

$$\mathbf{S} = \alpha^{-1}(\mathbf{C}^{-\alpha} - \mathbf{I}) \quad (3)$$

where \mathbf{C}^{-1} is the Finger strain tensor. In the case where a discrete relaxation spectrum is considered, the memory function becomes:

$$m(s) = \sum_i \frac{G_i}{\tau_i} \exp(-s/\tau_i) \quad (4)$$

where the τ_i are the relaxation times. In some studies¹⁷ the parameters G_i and τ_i have been determined in order to match the variations of the dynamic moduli with frequency. A precise enough adjustment usually requires between five and ten relaxation times.

Together with expression (4) of the memory function and the Finger strain tensor, the tensile stress may be easily calculated for a constant strain rate extensional test according to Eq. (1).¹⁸

If expression (3) is taken as the strain measure, one obtains the following relation for the true tensile stress measured during uniaxial extension at constant strain rate ($\sigma(t) = \sigma_{11}(t) - \sigma_{22}(t)$):¹⁹

$$\begin{aligned} \sigma(t) = 2 \sum_i \frac{\dot{\epsilon} G_i \tau_i}{1 - 2\alpha \dot{\epsilon} \tau_i} [1 - \exp(-(1 - 2\alpha \dot{\epsilon} \tau_i)t/\tau_i)] \\ + \sum_i \frac{\dot{\epsilon} G_i \tau_i}{1 + \alpha \dot{\epsilon} \tau_i} [1 - \exp(-(1 + \alpha \dot{\epsilon} \tau_i)t/\tau_i)] \end{aligned} \quad (5)$$

In a recent study on polystyrene melts,²⁰ we have shown that the tensile stress $\sigma(t)$ for a constant strain rate experiment can be approximated by the expression:

$$\sigma(t, \dot{\epsilon}) = \sigma_v(t, \dot{\epsilon}) + G(\dot{\epsilon}) \cdot (\lambda_r^2 - \lambda_r^{-1}) \quad (6)$$

where $\sigma_v(t, \dot{\epsilon})$ reaches a steady-state value $\sigma_v(\dot{\epsilon})$ after a relatively short time and where λ_r is the recoverable strain of the sample. Furthermore, it could also be shown that as a first approximation, the value of $\sigma_v(\dot{\epsilon})$ can be connected with polymer shear viscosity by the simple relation:

$$\sigma_v(\dot{\epsilon}) \sim 3 \cdot \dot{\epsilon} \cdot \eta(\dot{\gamma})|_{\dot{\gamma}=\dot{\epsilon}} \quad (7)$$

If we further assume that the first Cox-Merz relation is verified, that is, the value of the shear viscosity $\eta(\dot{\gamma})$ is close to that of the dynamic viscosity $\eta^*(\omega)$ for $\omega = \dot{\gamma}$,^{21,22,23} relation (7) can be rewritten in the form:

$$\sigma_v(\dot{\epsilon}) \sim 3 \cdot \dot{\epsilon} \cdot \eta^*(\omega)|_{\omega=\dot{\epsilon}} \quad (8)$$

Taking into account the two contributions to the stress arising in Eq. (6), we propose to describe the extensional rheological behaviour of the LDPE melts by a Maxwell model with two relaxation times.

Since the stress $\sigma_v(t, \dot{\epsilon})$ reaches a constant value $\sigma_v(\dot{\epsilon})$ and considering relation (8), we propose to describe it as a function of time by the following expression equivalent to a linear Maxwell model:

$$\sigma_1(t) = 3\dot{\epsilon} \cdot \eta^*(\omega) \cdot [1 - \exp(-t/\tau_0)]|_{\omega=\dot{\epsilon}} \quad (9)$$

$\eta^*(\omega)$ being the dynamic viscosity at $\omega = \dot{\epsilon}$.

The second term of Eq. (6) is similar to a rubber elasticity term and we hypothesize that it can be related to the deformation of the entanglement network.

For the sake of simplicity, we will try to fit this contribution to the stress by a non linear Maxwell model with only one relaxation time and therefore express it similarly to relation (5).

$$\begin{aligned} \sigma_2(t) = 2\dot{\epsilon} \frac{G \cdot \tau}{1 - 2a\dot{\epsilon}\tau} \{1 - \exp[-(1 - 2a\dot{\epsilon}\tau)t/\tau]\} \\ + \dot{\epsilon} \frac{G \cdot \tau}{1 + a\dot{\epsilon}\tau} \{1 - \exp[-(1 + a\dot{\epsilon}\tau)t/\tau]\} \end{aligned} \quad (10)$$

If $\dot{\epsilon}$ tends to 0 and t tends to infinity in the sum $\sigma_1(t) + \sigma_2(t)$ one obtains a further condition for the parameters of the model by writing Trouton's relation corresponding to the low strain-rate linear viscoelastic behavior:

$$\lim_{\substack{\dot{\epsilon} \rightarrow 0 \\ t \rightarrow \infty}} \left(\frac{\sigma_1(t) + \sigma_2(t)}{\dot{\epsilon}} \right) = 3\eta^*(\omega) \Big|_{\omega=\dot{\epsilon}} + 3 \cdot G \cdot \tau = 3\eta_0 \quad (11)$$

where η_0 is zero shear viscosity.

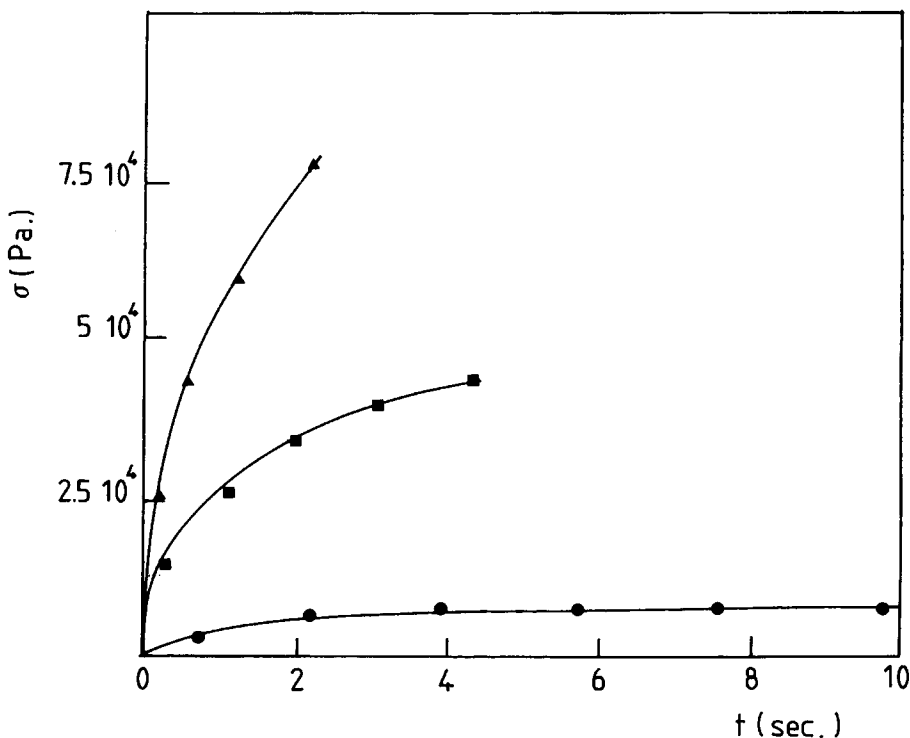


Fig. 8. Tensile stress as a function of time for the LL1 melt at 150°C and three different strain rates: (\blacktriangle) 1 s^{-1} ; (\blacksquare) $.5 \text{ s}^{-1}$; (\bullet) $.11 \text{ s}^{-1}$. (—) experimental curves; (\blacktriangle , \blacksquare , \bullet) calculated stress according to Eq. (12) with parameters α , τ_0 and τ from Table III.

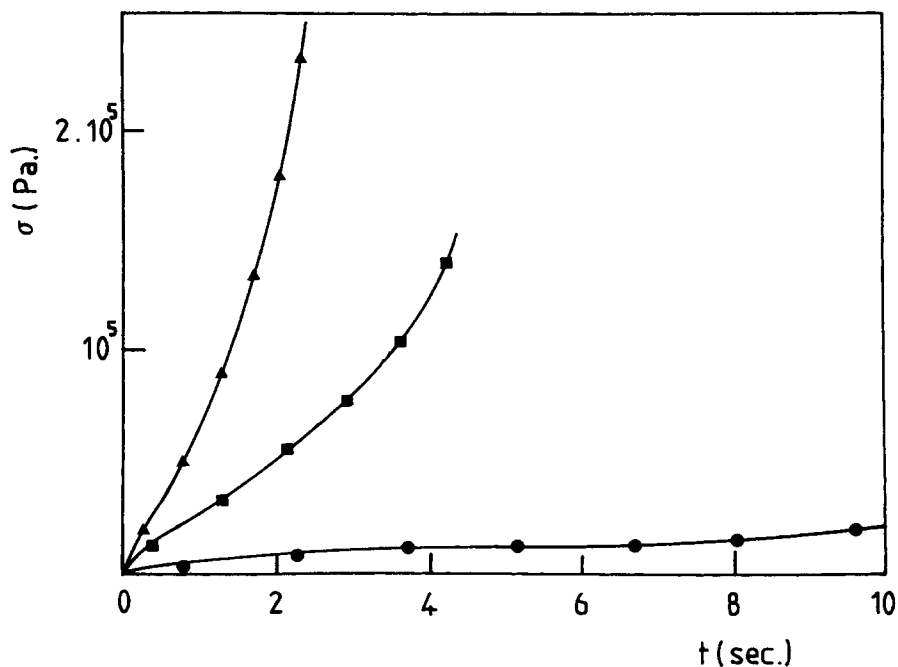


Fig. 9. Same representation than in Fig. 8 for the LD1 melt: (\blacktriangle) 1 s^{-1} ; (\blacksquare) $.5 \text{ s}^{-1}$; (\bullet) $.11 \text{ s}^{-1}$.

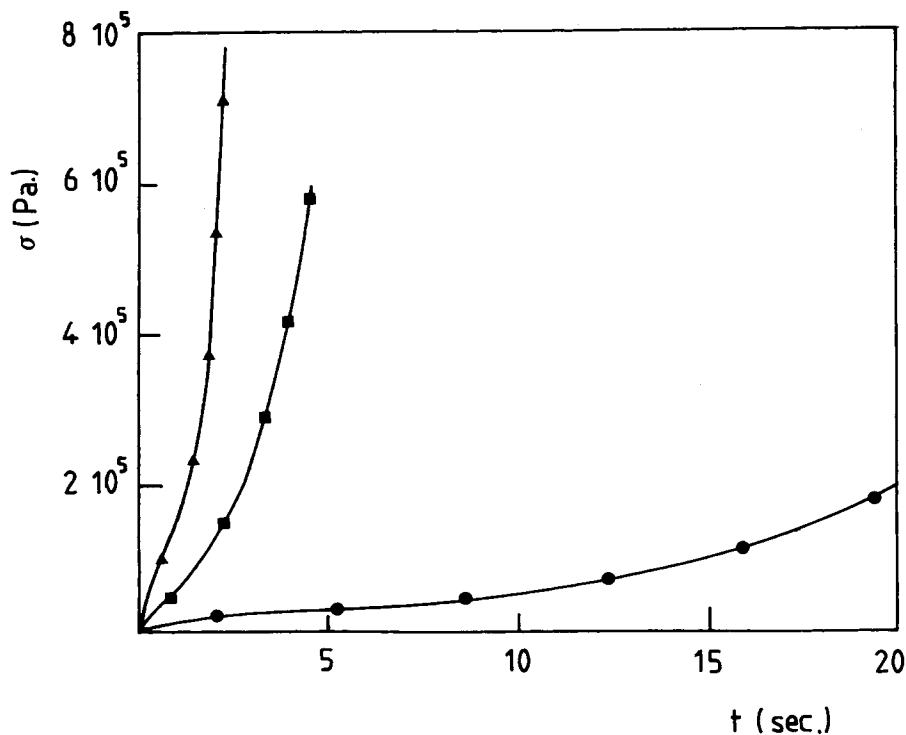


Fig. 10. Same representation than in Fig. 8 for the LD2 melt: (\blacktriangle) 1 s^{-1} ; (\blacksquare) $.5 \text{ s}^{-1}$; (\bullet) $.11 \text{ s}^{-1}$.

TABLE III
 Calculated Values of Parameters a , τ_0 , τ , G and G_0 of the Model,
 Giving the Best Fit of the Experimental Curves

	$\dot{\epsilon}$ (s^{-1})	a	τ (s)	G (pa)	τ_0 (s)	G_0 (Pa)
LD1	.055	1	21	6.6E2	2.8	1.6E4
	.11	.86	15	1.4E3	2.5	1.5E4
	.52	.74	8.3	4.2E3	1.1	2.0E4
	1	.74	6.5	6.2E3	.6	3.0E4
LD2	.03	.67	110	3.9E3	15	1.1E4
	.055	.66	100	4.7E3	10	1.3E4
	.11	.73	80	6.3E3	6	1.6E4
	.22	.72	75	7.0E3	3	2.4E4
	.52	.75	39	1.4E4	1.4	3.1E4
	1	.75	31	1.8E4	.6	4.9E4
LL1	.11	.76	13	1.6E2	1.1	2.1E4
	.52	.53	4.8	1.1E3	.45	4.5E4
	1	.47	2.8	2.7E3	.35	5.1E4

The final expression for the stress can therefore be written:

$$\sigma(t) = 3 \cdot \dot{\epsilon} \cdot \eta^*(\omega) \cdot [1 - \exp(-t/\tau_0)] + [\eta_0 - \eta^*(\omega)] \cdot \left\{ \frac{\dot{\epsilon}}{1 - 2a\dot{\epsilon}\tau} [1 - \exp(-(1 - 2a\dot{\epsilon}\tau)t/\tau)] + \frac{\dot{\epsilon}}{1 + a\dot{\epsilon}\tau} [1 - \exp(-(1 + a\dot{\epsilon}\tau)t/\tau)] \right\} \quad (12)$$

Since the values of η_0 and $\eta^*(\omega)$ can be determined from dynamic measurements in the linear range, only three independent parameters remain in Eq. (12): the two relaxation times τ_0 and τ , and the slip parameter a .

A least-square regression program has been used to determine these parameters from the experimental curves. The calculation has been carried out by a succession of approximations on ten experimental points chosen on the curve.

As can be seen in Figures 8, 9, and 10, the model proposed fits the experimental stress-growth curves for three samples and for various strain rates. In Table III, we have listed the calculated values of the three parameters a , τ and τ_0 which lead to the best agreement between the model and the experiment.

DISCUSSION

Parameter τ_0

Relaxation time τ_0 related to σ_1 contribution to the stress is on the whole smaller than the second relaxation time by a factor of 10. It can also be noticed that τ_0 decreases if the strain rate is increased and that for most tests

on the branched melts (LD1 and LD2), the product $\dot{\epsilon} \cdot \tau_0$ remains approximately constant, its value being about 0.6; this indicates that σ_1 contribution to the stress is associated to short time relaxation processes which depend on deformation rather than on the strain rate.

Parameter τ

In Lodge's theory,^{24,16} one considers segments of chains between two entanglements and with a number j of monomer units. If the disentanglement probability of these segments is $1/\tau_i$ and their rate of formation G_i/τ_i expression (4) of the memory function is obtained.

In our approach, considering only one relaxation time in expression 10 of $\sigma_2(t)$, leads to the assumption that all segments between entanglements have the same length. This is obviously only a first approximation and the further interpretation of a , τ , and G and their variation with strain rate will have only a qualitative meaning.

Generally, the quantity G , which has the dimension of a modulus and is related to the number of segments of the entanglement network, increases if the strain rate is increased, whereas the relaxation time decreases under the same conditions.

A possible interpretation of these variations with strain rate consists in assuming that the number of entanglements which effectively contribute to the stress depends on the strain rate and increases if the latter is increased. At the same time, the average length of the chain segments between these entanglements decreases, and so does their disentanglement time.

A comparison of the behavior of the three samples shows that the values of G and τ are higher for the branched polymers at the same strain rate. From the previous observations, it seems that the influence of the long chain branching is to increase the number of effective entanglements as well as their life-time.

It can be seen that this effect is more perceptible for the LD2 melt which has an average molecular weight comparable to that of the LD1 melt but which has a lower long chain branching extent and therefore a higher average length of branches. This would mean that for branched polymers, the length of the branches plays an important role on the extensional rheological behaviour by decreasing significantly the disentanglement probability of the chains.

Parameter a

The so-called slip parameter of entanglements introduced in the model, the value of which lies between 0 and 1, accounts for nonaffine deformation of the entanglement network.

It can be seen that for samples LL1 and LD1, the value of a determined by fitting the experimental curves decreases if the strain rate is increased, whereas it is almost independent of strain rate for the sample LD2 ($a \approx .7$).

A qualitative interpretation of this result can be given by saying that if the strain rate increases, the number of entanglements taken into account in the model increases and their average relaxation time decreases. As a whole, these

entanglements become weaker and it can reasonably be assumed that the deformation of their network becomes less affine.

If samples LL1 and LD1 are compared, it can be seen that the long-chain branching increases the value of a for the same strain rate and, therefore, the slipping of entanglements decreases. The fact that a is almost strain rate independent for the LD2 sample is more difficult to explain. The relatively small value of a does not seem to be in agreement with the high values of the relaxation times. It seems likely that the influence of the number of long-chain branches and of their length is not the same on the slip parameter and on the relaxation times.

CONCLUSION

In this study we were able to show that in a strain rate range between $.03 \text{ s}^{-1}$ and 1 s^{-1} and for Hencky strains up to 2.5, the tensile stress-growth coefficient of linear and branched LDPE melts could be described as a function of time by a simple model with two relaxation times.

For this purpose it has been assumed that the tensile stress arises from two contributions. The first one can be fitted by a linear Maxwell model in which the dynamic viscosity of the polymer occurs. The second one is ascribed to the entanglement network and can be fitted by a nonlinear Maxwell model which can account for a nonaffine deformation of the junction points between the chains. The three adjustable parameters of the model are the two relaxation times and the slip parameter of entanglements.

The effect of the structure of the chains on the relaxation times seems to be consistent but a better understanding of the variations of the slip parameter would require more experiments on polymers with a better controlled molecular weight distribution and structure (monodisperse star or comb-shaped molecules). These would presumably allow better separation of the respective influence of number and length of branches.

The authors would like to thank the CDF Chimie Company, Mazingarbe, France, for financial support and for providing the samples.

References

1. C. D. Han, Y. J. Kim, H. K. Chuang, and T. H. Kwack, *J. Appl. Polym. Sci.*, **28**, 3435 (1983).
2. G. Attalla and F. Bertinotti, *J. Appl. Polym. Sci.*, **28**, 3503 (1983).
3. D. R. Saini and A. V. Shenoy, *Polym. Eng. Sci.*, **24**, 1215 (1984).
4. T. Raible, A. Demarmels, and J. Meissner, *Polym. Bull.*, **1**, 397 (1979).
5. H. M. Laun and H. Munstedt, *Rheol. Acta*, **17**, 415 (1978).
6. H. M. Laun and H. Munstedt, *Rheol. Acta*, **15**, 517 (1976).
7. M. H. Wagner, *Rheol. Acta*, **15**, 136 (1976).
8. F. P. La Mantia and D. Acierno, *Polym. Eng. Sci.*, **25**, 279 (1985).
9. H. Munstedt and H. M. Laun, *Rheol. Acta*, **20**, 211 (1981).
10. R. Muller and D. Froelich, *Polymer* **26**, 1477 (1985).
11. F. T. Trouton, *Proc. Roy. Soc.*, **A77**, 426 (1906).
12. H. Munstedt and H. M. Laun, *Rheol. Acta*, **18**, 492 (1979).
13. M. Doi and S. F. Edwards, *J. Chem. Soc. Faraday Trans. II*, **74**, 1789, 1802, 1818 (1978).
14. N. W. Tschoegl, *Polymer*, **20**, 1365 (1979).
15. M. W. Johnson, Jr. and D. Segalman, *J. Non-Newtonian Fluid Mech.*, **2**, 255 (1977).
16. C. J. S. Petrie, *J. Non-Newtonian Fluid Mech.*, **5**, 147 (1979).

17. M. H. Wagner, *J. Non-Newtonian Fluid Mech.*, **4**, 39 (1978).
18. C. J. S. Petrie, *Elongational Flows*, Pitman, London, 1979.
19. H. Janeschitz-Kriegl, *Polymer Melt Rheology and Flow Birefringence*, Springer Verlag, Berlin, 1983.
20. R. Muller, D. Froelich, and Y. H. Zang, *J. Polym. Sci., Polym. Phys. Ed.*, to be published.
21. H. C. Booij, P. Leblans, J. Palmen, and G. Tiemersma-Thoone, *J. Polym. Sci., Polym. Phys. Ed.*, **21**, 1703 (1984).
22. R. N. Shroff and M. Shida, *J. Polym. Sci. A2*, **8**, 1917 (1970).
23. M. H. Wagner and J. Meissner, *Makromol. Chem.*, **181**, 1533 (1980).
24. A. S. Lodge, *Elastic Liquids*, Academic Press, New York, 1964.

Received January 28, 1986

Accepted June 7, 1986